



HAL
open science

State-of-the-Art of Pressure Drop in Open-Cell Porous Foams: Review of Experiments and Correlations

Prashant Kumar, Frederic Topin

► **To cite this version:**

Prashant Kumar, Frederic Topin. State-of-the-Art of Pressure Drop in Open-Cell Porous Foams: Review of Experiments and Correlations. *Journal of Fluids Engineering*, 2017, 139 (11), 10.1115/1.4037034 . hal-01792826

HAL Id: hal-01792826

<https://hal.science/hal-01792826>

Submitted on 20 Feb 2023

HAL is a multi-disciplinary open access archive for the deposit and dissemination of scientific research documents, whether they are published or not. The documents may come from teaching and research institutions in France or abroad, or from public or private research centers.

L'archive ouverte pluridisciplinaire **HAL**, est destinée au dépôt et à la diffusion de documents scientifiques de niveau recherche, publiés ou non, émanant des établissements d'enseignement et de recherche français ou étrangers, des laboratoires publics ou privés.

State-of-the-Art of Pressure Drop in Open-Cell Porous Foams: Review of Experiments and Correlations

Prashant Kumar¹

IUSTI,
CNRS UMR 7343,
Aix-Marseille Université,
Marseille 13284, France;
Technopole de Château Gombert,
5, Rue Enrico Fermi,
Marseille Cedex 13 13453, France
e-mail: prashant.kumar@etu.univ-amu.fr

Frédéric Topin

IUSTI,
CNRS UMR 7343,
Aix-Marseille Université,
Marseille 13284, France;
Technopole de Château Gombert,
5, Rue Enrico Fermi,
Marseille Cedex 13 13453, France
e-mail: frederic.topin@univ-amu.fr

Foam structures are a class of modern microporous media that possesses high thermal conductivity, large accessible specific surface area, and high porosities. Nowadays, industrial applications, such as filtration, heat exchange and chemical reaction, etc., utilize porous media such as open-cell foams. Knowledge of pressure drop induced by these foam matrices is essential for successful design and operation of high-performance industrial systems. The homogenized pressure drop data in the literature are widely dispersed (up two orders of magnitude) despite numerous researches has been conducted since two decades. Most of the empirical pressure drop correlations were derived using Ergun-like approach. In this view, a careful evaluation of empirical correlations as well as the relationship of intrinsic flow law characteristics (permeability and inertia coefficient) with morphological parameters is imperative. This paper presents the start-of-the-art of various pressure drop correlations as well as highlights the ambiguities and inconsistencies in various definitions of several key parameters. The applicability of the empirical correlations presented in the literature was examined by comparing them against numerically calculated pressure drop data of open-cell foams (metal and ceramic) for the porosities ranging from 0.60 up to 0.95. A comprehensive study has been conducted to identify the reasons of dispersed pressure drop data in the literature. Although substantial progress has been made in the field of fluid flow in open-cell foams, it is yet difficult to predict pressure drop data from a given set of morphological parameters.

1 Introduction

Open-cell foam is a cellular material defined by roughly ellipsoidal voids surrounded by a three-dimensional (3D) network of solid (see Fig. 1). As a lightweight porous material, open-cell foam possesses a high strength and stiffness relative to its weight, making it an attractive option for a variety of applications. Open-cell foams can be manufactured from several metals and alloys, e.g., aluminum, copper, steel, and nickel [1], and ceramics, e.g., Al_2O_3 , Mullite, SiC, and OBSiC [2–5] using various manufacturing processes, such as casting, replication by electro-deposition, mold infiltration, etc.

In the applications requiring flow of liquid or gas in open-cell foams, e.g., heat exchangers, filters, catalysis support, etc., understanding of various flow regimes in such foams, and the associated pressure drop is critical [6–13]. In the case of heat exchangers or reactor designing, studying pressure drop is crucial to identify fan power requirement and a design goal is to minimize this power expenditure [4,14]. The efficiency of these industrial processes depends on the permeability of the porous medium employed. Therefore, it is very important to understand the fluid flow dynamics through porous medium as well as the methods to calculate its permeability or the pressure drop properties [2–5,9–16]. Many researchers performed experiments with open-cell foams (metal and ceramic) in order to pursue a complete characterization of this kind of materials with easily accessible and measurable morphological parameters. Morphological parameters (e.g., pore or strut diameter, porosity, specific surface area, etc.) of a foam structure

are interlinked with each other and yet are still not well understood. They impact very strongly on flow law characteristics (permeability and inertia coefficient), and thus, more efforts are

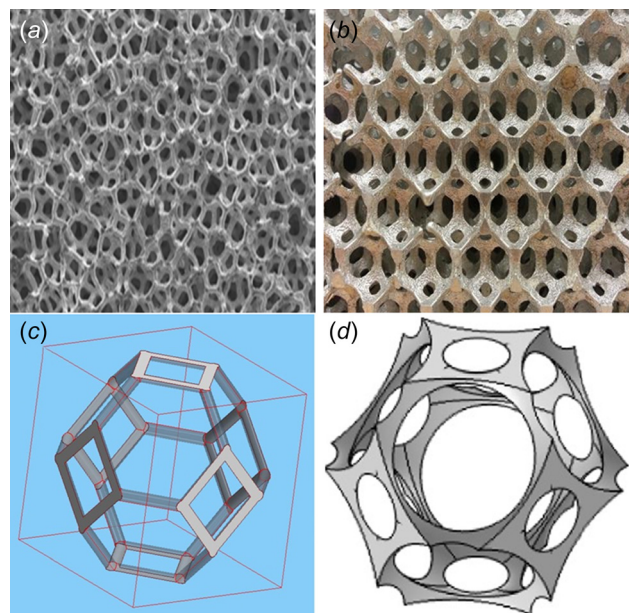


Fig. 1 Examples of open-cell foams: (a) commercial replication method sample, (b) sand casted sample, ((c) and (d) two examples of isotropic idealized Kelvin-like unit cell: (c) circular strut assembly along truncated octahedron skeleton and (d) sphere subtracted from solid truncated octahedron

needed in order to fully understand the behavior of these materials in fluid flow applications.

Usually, two fluid flow regimes are distinguished in open-cell foams. Viscous flow is characterized by a symmetrical flow pattern over a unit cell, while it becomes asymmetrical in the inertia regime. It is important to note that inertia effect is very weak in viscous regime, while viscous effect is very weak in inertia regime. Thus, permeability and inertia coefficient are important parameters for the characterization of foams employed in industrial applications. Note that all flow law equations (in one-dimensional form) of the fluid involved inside the porous medium or open-cell foams (Eqs. (1)–(4)) are given for the case of constant thermo-physical properties (e.g., viscosity) and incompressible fluid.

Darcy's law is a generalized relationship for viscous flow in porous media. It is a simple proportional relationship between the instantaneous discharge rate through a porous medium, the viscosity of the fluid, and the pressure drop over a given distance and is given by the following equation:

$$\frac{\Delta P}{\Delta x} = \frac{\mu}{K_D} V \quad (1)$$

where ΔP is the pressure drop along the length Δx of the medium, K_D is the intrinsic permeability of the porous medium, μ is the viscosity of fluid, and V is the superficial fluid velocity.

Experimentally, the linearity of the relationship between the pressure drop ($\Delta P/\Delta x$) and superficial velocity (V) is checked only at low Reynolds numbers where flow is laminar. This model is particularly useful in the field of hydrogeology where flow takes place in low-porosity porous medium (< 0.5). However, as soon as the flow velocity increases, nonlinear effects start appearing, and then, this model has its limitations for the description and prediction of pressure drop.

It is well known that the pressure drop during one-dimensional flow through a packed bed (or open-cell foams) of granular material is given by the sum of two terms: a viscous energy loss term and an inertial loss term and it is well described by Forchheimer equation

$$\frac{\Delta P}{\Delta x} = \frac{\mu}{K_D} V + C_{\text{For}} \rho V^2 \quad (2)$$

where C_{For} is the inertia coefficient and ρ is the fluid density.

However, a few authors (e.g., see Refs. [17] and [18]) have shown that the onset of the nonlinear behavior (which is sometimes called the weak inertia regime) can be described by a Cubic law

$$\frac{\Delta P}{\Delta x} = \frac{\mu}{K_D} V + \frac{\gamma \rho^2}{\mu} V^3 \quad (3)$$

where γ is a dimensionless parameter for the nonlinear term. $C_{\text{For}}(V) = (\gamma \rho/\mu)V$ can be described as a velocity-dependent inertial coefficient.

For a range of Reynolds number based on pore diameter ($\text{Re} = \rho V d_p/\mu$) tested (low and high Re), there is an occurrence of Cubic law (see Eq. (3)) as a transition regime in the case of periodic foams as Kumar and Topin [11] have shown. Transition regime occurs at a slight departure from the viscous regime where the flow pattern starts to become asymmetrical. Experimentally, the probability of occurrence of Cubic Law is very low in the case of nonperiodic foams as it is very difficult to control the velocity during the experiments. Transition regime occurs between viscous and inertia regimes in a very narrow Reynolds number range and its visibility is generally suppressed by the inertia regime. Thus, fluid flow using cubic law in porous media is generally not reported in the literature.

The most widely accepted interpretation of the Forchheimer equation was presented by Ergun and Orning [19]. These authors adopted the Forchheimer equation and introduced a

morphological parameter similar to those used for packed beds of spheres to express pressure drop (see Eq. 4). However, this relation is very popular to derive empirical correlations in case of open-cell foams

$$\frac{\Delta P}{\Delta x} = E_1 \frac{(1 - \varepsilon_o)^2}{\varepsilon_o^3} \frac{1}{D_p^2} \mu V + E_2 \frac{(1 - \varepsilon_o)}{\varepsilon_o^3} \frac{1}{D_p} \rho V^2 \quad (4)$$

where E_1 and E_2 are the coefficients of the viscous and inertial terms, D_p (equivalent particle diameter), and ε_o (porosity) are morphological parameters, respectively.

Numerous experimental studies on pressure drop in open-cell foams have been conducted in the literature where authors usually reported the flow law characteristics (permeability and inertia coefficient). However, none of the authors discussed and identified the bias, quality, and accuracy of the pressure drop data that depend on how the experiments have been performed. The basic question that comes up here is how the pressure drop (or pressure gradient, ∇P) has been measured by different authors. Moreover, various empirical correlations (e.g., see Refs. [2–5], [8], [11–13], and [20–33]) were also proposed in the literature. These correlations were mainly derived using Ergun-like approach (Eq. (4)). Depending on the author's definitions and set of morphological data, various versions of Ergun-like approaches have been used in the literature.

Plotting the dimensionless pressure drop data in the form of friction factor (f) against Reynolds number (Re) generally called a Moody diagram is the usual way to distinguish different flow regimes. A characteristic length (C_L) is sufficient to obtain the qualitative trend of friction factor in different flow regimes (Eq. (5)). Friction factor is calculated by determining pressure drop across the foam sample and is given as:

$$f = \frac{\Delta P}{\Delta x} \frac{C_L}{\rho V^2} \quad (5)$$

where C_L is characteristic length scale.

This characteristic length (C_L) could be either a morphological (e.g., hydraulic diameter, $d_h = 4\varepsilon_o/a_c$) or a flow law characteristics parameter (e.g., square root of Darcian permeability, $\sqrt{K_D}$). However, the choice of the characteristic length to obtain quantitative friction factor that could be applied on different foam samples used by different authors is still unclear in the literature.

Bonnet et al. [16] showed that at fixed pore size, pressure loss generated by the foam disperses over two orders of magnitude for low velocity, and one order of magnitude for high velocity. This dispersion in the data could be easily related to: (1) the choice of the flow law, i.e., Darcy, Forchheimer and Cubic laws to extract flow law characteristics, (2) inconsistencies between the definitions of characteristic length scale and morphological parameters, and (3) compressibility effect for gas fluid flow.

The objective of the present work is to critically analyze:

- Bias in experimental pressure drop measurements.
- Data treatment and extraction of flow law characteristics (permeability and inertia coefficient).
- Analysis of different characteristic length scales.
- Validity and applicability of proposed literature correlations.

2 Literature Review and Analysis of Pressure Drop Experiments and Correlations

This section is divided into two parts: (1) pressure drop data and data treatment to deduce flow law characteristics (permeability and inertia coefficient) and (2) correlations for modeling pressure drop versus flow rate as a function of foam characteristics. For a studied Reynolds number range, it is a common practice to extract the flow law characteristics by fitting the data on first-, second-, or third-order polynomial curve.

2.1 Monophasic Flow Experiments in Open-Cell Foams.

The pore space in foams constitutes of roughly ellipsoidal

interconnected cells. Each cell is connected to ten up to 17 neighbors. Usually, the contact space between two adjacent cells is called a window. In contrast to a common argument reported in the literature, the pore space is not tortuous; fluid tortuosity of open-cell foam is close to 1 [34–37]. The flow in such media is more characteristic of a flow around many obstacles with a repeated disruption of hydrodynamic boundary layers than the usual description of flow in tortuous tubes linked together by constrictions. The flow may recirculate at the back of the solid struts and, sometimes, unsteady flow (or even turbulence) occurs [38]. The geometric complexity prevents exact solutions of the transport equations inside the pores (see Refs. [39–41]). This led researchers to rely heavily on pressure drop experiments (e.g., see Refs. [2–5], [8], and [42–45] etc.).

Several authors measured pressure drop just by measuring pressure in the upstream and downstream of their foam samples (e.g., see Dietrich et al. [3], Inayat et al. [4], Liu et al. [30], Dukhan [32], Dukan and Patel [46], Mancin et al. [47]). These authors performed steady-state, unidirectional, and static pressure drop experiments, as for example in an open-loop wind tunnel or using a flow distributor in front of the sample. The pressure was measured using pressure taps/sensors located before and after the foam sample of the test section for different flow velocities.

Some authors (e.g., see Bonnet et al. [16], Topin et al. [31], Madani et al. [48]) used a different strategy to obtain the pressure profiles along the length of the flow axis and captured the entrance and the exit effects. These authors used different pressure sensors implanted in the foam samples and uniformly spaced along the main flow axis. Such an experimental setup allows separating the inlet and outlet effects and reconstructing the established pressure gradient along the main flow axis (representative of the flow in an “infinite” medium).

Note that most of the experiments used air or water at room temperature as working fluid in open-cell foams. Only a few authors measured precisely the fluid properties variation and used gas as working fluid to take into account the compressibility effect during data extraction (see detailed discussions in Bonnet et al. [16] and Madani et al. [48]).

Several authors (see Refs. [10–12], [49], and [50]) have performed direct pore scale numerical simulation on actual (reconstructing 3D foam structure obtained from μ CT scanned images) or simplified foam structures (Kelvin-like or Weaire–Phelan foam structures) to obtain flow law characteristics. Accuracy of the results is usually associated with high-quality scans of existing foam samples. In this case, exact pressure at the entrance and exit as well as pressure profile along the sample length can be easily obtained to compute pressure drop and pressure gradient.

For designing various reactors, heat exchangers, etc., flow law characteristics and pressure drop in open-cell foams are crucial [14]. It can be easily observed in the literature that the individual data are not deduced in a consistent manner by authors. This is due to the measurement inconsistencies as well as data extraction of flow law characteristics data from the experiments [48].

Most commonly, the flow law characteristics (permeability and inertia coefficient) were deduced by fitting the second-order polynomial pressure drop data versus velocity. In most of the cases, the regimes were not identified as Reynolds number was always assumed to be in weak inertia regime. On the other hand, deducing flow law characteristics data in this manner lead to different results because these characteristics depend on the velocity range. Permeability obtained by fitting pressure drop data to a second-order polynomial curve is actually Forchheimer permeability (K_{For}) and vary with velocity range. This explains the fact why similar foam structures exhibit different permeability values. On the other hand, inertia coefficient values (C_{poly}) obtained from fitting data are accurately measured.

Dukhan and Minjeur [9] presented that the extraction of permeability from linear pressure drop ($\Delta P/\Delta x$) versus velocity (V) data yields an apparent value of Forchheimer permeability (K_{For}) that is sensitive to the velocity range and is different from the Darcian

permeability (K_D). The authors experimentally showed that the determination of permeability and inertia coefficient using polynomial fitting possibly mixes flow regimes, i.e., Darcy, transitional, and Forchheimer regimes, which lead to errors in flow law characteristics.

Kumar and Topin [11,12] numerically calculated pressure gradient and velocities in viscous and inertia regimes on virtual foam samples for various strut cross sections. The authors identified the different flow regimes to choose the flow law based on the methodology proposed by Firdaouss et al. [51] that was based on a normalization technique of pressure drop, velocity, and permeability. In their work, flow regimes were clearly distinguished using symmetry property of the flow pattern. Viscous regime was identified as symmetrical flow pattern, while a slight departure from the symmetry indicated transition regime. Weak inertia regime was characterized by asymmetrical flow pattern. The authors deduced Darcian permeability (K_D) and Forchheimer inertia coefficient (C_{For}). The authors also showed that it was possible to trace back the same values of computational fluid dynamics (CFD) numerical pressure drop data using K_D and C_{For} .

Other sources of inconsistencies in pressure drop data come from the definitions and measurements of morphological parameters to be used as a characteristic length scale in characterizing $f - \text{Re}$ relationship of open-cell foams [16]. This relationship is widely scattered in the literature and arises mainly due to the different choices of morphological parameters (e.g., D_p , d_p , d_h) to be employed in characteristic length scale. This length scale is usually linked to flow regime (viscous, transition, or inertia regime) and may change depending on the kind of the parameters employed. Moreover, ambiguities in definitions and measurements of these length scales vary from one author to another.

A first group of authors (e.g., see Inayat et al. [4], Liu et al. [30], Beugre et al. [52]) used equivalent particle diameter (D_p) by using the analogy between solid foam and spherical particles with the same specific surface area per unit volume and the same porosity. The second group of authors (e.g., see Richardson et al. [23], Boomsma et al. [49]) used pore diameter (d_p) as a characteristic length scale, while the third group of authors (e.g., see Dietrich et al. [3], Kumar and Topin [12], Bonnet et al. [16]) used hydraulic diameter (d_h) as a characteristic length scale.

Many authors [4,20,22,29,33] defined equivalent particle diameter by simply using the classical formula that relates specific surface area (a_c), porosity (ε_0), and a particle sphere diameter (D_p), leading to $D_p = 1.5d_s$ or $D_p = 6(1 - \varepsilon_0)/a_c$. Cellular materials like open-cell foams do not comply with the same geometry as packed bed of spherical particles, and thus, such a relation will not hold because pore size and pore density changes with the manufacturing processes (also see Dukhan and Patel [46]). These analogous relations inhibit significant error in pressure drop correlations and, thus, cannot be applied directly to the open-cell foams.

Pore diameter is most widely used as the characteristic length scale to characterize the $f - \text{Re}$ relationship because of the well-defined solid structure of foams (see Boomsma et al. [49], Mancin et al. [47]). Pore diameter was preferred as it is relatively easy to measure from 3D tomography images (see Vicente et al. [53]) in open-cell foams. Edouard et al. [54] showed that the use of the pore diameter (d_p) of the foam as a characteristic length was not appropriate by comparing a large set of correlations and experimental data from the literature. It is due to several definitions to estimate pore diameter that leads to arise inconsistencies when comparing different data from the literature. Generally, the definition and measurement of pore diameter is not similar and varies according to the author and the tool used. Using 3D scanned images, pore diameter could be defined as average diameter of disks of same areas than average opening window as pore diameter [55] or it could be defined as diameter of sphere of same volume as pore diameter [11]. Some authors (e.g., see Mancin et al. [47]) even used the expression as 25.4/pores per linear inch (in mm) as pore diameter. This could be more troublesome if pore

diameter was estimated from the distribution over several thousand extracted pores of a 3D image (e.g., see Inayat et al. [4]) over a dozen of handmade measurements on a two-dimensional image (e.g., Richardson et al. [23]).

Several authors expressed their natural interest in using hydraulic diameter, $d_h = 4\varepsilon_0/a_c$ (e.g., see Dietrich et al. [3], Kumar and Topin [12]) as a characteristic length scale. Hydraulic diameter constitutes both porosity and specific surface area and, thus, includes the impact of strut shape. These parameters are purely structural parameters that can be measured. Fluid flow inside pore space depends on strut shape and interconnected ligaments but not explicitly on specific surface area in Darcy regime. However, the nature of the strut (hollow or solid) induces inconsistencies in obtaining specific surface area. This depends on the method applied, e.g., Brunauer–Emmett–Teller (BET) (e.g., see Richardson et al. [23]) method or magnetic resonance imaging (e.g., see Dietrich et al. [3]) technique. In recent times, specific surface area is also obtained by reconstructing 3D foam structure from μ CT scanned images. However, accuracy of the results is associated with the quality scans of existing foam samples. Moreover, Kumar and Topin [11] showed that flow law characteristics are strut shape dependent and could exhibit different results for a given pore size of foam samples.

Due to the several inconsistencies in measurements and various definitions of morphological parameters used by different authors, it has also been proposed to use directly the square root of permeability ($\sqrt{K_{For}}$), which has the dimension of a length and contains information about the viscous part of flow law (e.g., see Paek et al. [43], Boomsma and Poulikakos [15], Xu et al. [55], Dybbs and Edwards [56], Lage and Antohe [57]). The permeability obtained in the Darcy regime represents the actual internal structure of the porous medium most accurately that could be used to establish $f - Re$ relationship, thereby, reducing the ambiguities in definitions and measurements of morphological parameters and taking the internal 3D foam structure. However, usage of this length scale is limited as the viscous effects (or permeability) in experiments are not accurately measured [9,11,12,48] as it is Forchheimer permeability and is different from the one obtained in the Darcy regime. To eliminate such ambiguities in permeability, some authors calculated permeability in viscous regime [9,11,12] which allows using the square root of Darcian permeability ($\sqrt{K_D}$) as a characteristic length. However, this statement raises a new question of determining a different characteristic length that would describe the inertia regime well. Bonnet et al. [16] argued against the use of such expressions as characteristic lengths because they account only for Darcy flows. $\sqrt{K_D}$ as a characteristic length contains invisibly the information of strut shape and describe $f - Re$ relationship only in the Darcian regime. In the inertia regime, the problem arises due to constant and variable values of form drag coefficient (c_F). Some authors claimed c_F to be a so-called “universal” constant whose value was fixed for open-cell foams. The experimental reported values of c_F for high (and very close) porosity foam samples were from 0.0567 to 0.105 (see Dukhan and Minjeur [9], Paek et al. [43], Mancin et al. [47]). On the other hand, it was shown by many authors (see Kumar and Topin [11,12], Xu et al. [53], Lage and Antohe [57]) that the variety of constant c_F values appearing in friction factor correlations reflects the different inertial effects corresponding to different porosity at fixed cell size. The relative variation between these c_F values is about 50% for very similar foam samples. It clearly shows that c_F depends strongly on foam morphology and is very sensitive to porosity range (mainly low porosity) and, thus, could not be a “universal constant.”

The current analysis reveals the reasons of the dispersed pressure drop data (or friction factor data) by a two orders of magnitude. It can be summarized as follows:

- Pressure drop through open-cell foams is not measured in a consistent manner.
- Data extraction and treatment methods differ between authors.

- No general agreement is obtained on definitions and usage of morphological and flow law characteristics.
- Authors choose different characteristic length scales.

A comprehensive experimental/numerical flow law characterization of open-cell foams can be time consuming and expensive. Empirical correlations (based on experimental or CFD numerical data) have proved to be a quite efficient way of predicting pressure drop data using easily measurable morphological parameters of different foam samples without performing experiments. This led many authors to derive the correlations mainly based on an Ergun-like approach to introduce morphological parameters in order to obtain a reliable relationship with flow law characteristics.

The present analysis suggests that the pressure drop data, methodology of data extraction, and characteristic length scale choice are widely dispersed. This leads to a large scattering of reported flow law characteristics (permeability, inertia coefficient, and friction factor). Thus, it is critical to check the validity and applicability of correlations reported in the literature.

2.2 Correlations for Pressure Drop Prediction. In the literature, several authors have proposed various correlations based on Ergun-like approach (see Table 1) for the pressure drop prediction [2–5,8,11–13,20–33]. Table 1 summarizes the principal correlations available in the literature. Some authors (e.g., see Lacroix et al. [20]) have even used the coefficients of E_1 (=150) and E_2 (=1.75), which were actually determined for packed bed system. On the other hand, several authors (e.g., see Dietrich et al. [3], Lu et al. [21], Moreira et al. [26]) determined values of E_1 and E_2 for various set of foam samples of different pore sizes. Constant values of E_1 and E_2 were reported by these authors. Note that the constant values of E_1 and E_2 do not agree between authors and differ from the original values of the Ergun coefficients.

Several authors argued against the use of constant values of coefficients E_1 and E_2 . Values of E_1 and E_2 resulting from these approaches and used in these correlations are ranging typically between 100 and 865 and 0.65 and 2.65, respectively (e.g., see Inayat et al. [4], Tadrist et al. [8], Kumar and Topin [11,12], Richardson et al. [23]). On the other hand, some authors (e.g., see Dukhan [32], Mancin et al. [47]) tried to correlate flow law characteristics with morphological parameters of foam structure and did not use Ergun-like approach.

The validity and applicability of many correlations (e.g., see Refs. [8], [21], [23], [24], [29], [31], [32], and [58]) have already been discussed in the work of Edouard et al. [55] and, thus, are not discussed in detail in the present work. These authors [55] concluded that it appears that *no model is perfect and that the standard deviation between experimental and theoretical values can be as high as 100%*. The main limitation of these correlations is that they cannot be applied to an arbitrary chosen set of foam samples. Moreover, over-simplification of strut shape and size as well as definitions and “tools” to measure morphological properties and measurement accuracy issues are also some serious limitations for these large spreads in proposed empirical pressure drop models.

In the present work, we chose and analyze different arbitrary correlations for the comparison in the following paragraphs. Correlations from the recent works that include Ergun parameters, impact of strut shape on flow law characteristics, are extensively discussed.

Some authors (e.g., see Dukhan [32], Mancin et al. [47]) have even correlated pressure drop with PPI (pores per inch). Pores per inch does not give any reliable information about the cell size and is quoted by manufacturer (see Inayat et al. [4], Vicente et al. [54]), and thus, it is not suitable to derive or correlate to flow law characteristics. Dukhan [32] and Mancin et al. [47] presented a correlation to predict that pressure drop with PPI and, thus, may not be appropriate to other set of foam samples. These authors did not measure pore diameter but estimated pore diameter according to simple relation of 2.54/PPI (in mm). Mancin et al. [47]

Table 1 State-of-the-art correlation for predicting the pressure drop in open-cell foams

References	Sample	PPI	$d_p \times 10^{-3}$ (m)	ε_o	$K \times 10^{-8}$ (m ²)	C (m ⁻¹)	Correlation for pressure drop prediction
Lu et al. [21]	—	—	—	—	—	—	$f = \left[0.044 + \frac{0.008(d_p/d_s)}{(d_p/d_s - 1)^{0.43+1.13(d_s/d_p)}} \right] \text{Re}^{-0.15}$ $\text{Re} = \frac{\rho d_s (\nu/1 - d_s/d_p)}{\mu}$
Innocentini et al. [22]	30 PPI 45 PPI 60 PPI 75 PPI	30 45 60 75	0.928 1.28 0.291 0.161	0.89 0.88 0.85 0.85	3.20 2.56 0.51 0.39	1587.3 1176.4 5555.5 10,000	$f = 1.75 + 150 \frac{(1 - \varepsilon_o)}{\text{Re}}; \text{Re} = \frac{\rho D_p V}{\mu} \text{ with } D_p = 1.5 d_p \frac{(1 - \varepsilon_o)}{\varepsilon_o}$ $\frac{\Delta P}{\Delta x} = 150 \frac{(1 - \varepsilon_o)^2 \mu V}{\varepsilon_o^3 D_p^2} + 1.75 \frac{(1 - \varepsilon_o) \rho V^2}{\varepsilon_o^3 D_p}$
Richardson et al. [23]	Al ₂ O ₃ Al ₂ O ₃ Al ₂ O ₃ Al ₂ O ₃	10 30 45 65	1.68 0.826 0.619 0.359	0.878 0.874 0.802 0.857	1.92 0.482 0.396 0.239	122.82 431.03 876.55 1948.2	$\frac{\Delta P}{\Delta x} = \frac{E_1}{36} \frac{1}{\varepsilon_o^3} a_c^2 \mu V + \frac{E_2}{6} \frac{1}{\varepsilon_o^3} a_c \rho V^2$ $E_1 = 973 d_p^{0.743} (1 - \varepsilon_o)^{-0.0982}$ $E_2 = 368 d_p^{-0.7523} (1 - \varepsilon_o)^{0.07158}$
Du Plessis et al. [58]; Fourie and Du Plessis [24]	45 PPI 60 PPI 100 PPI 100 PPI	45 60 100 100	0.87 0.42 0.25 0.25	0.978 0.975 0.973 0.973	1.67 0.794 0.234 0.181	775 1014 2146 3090	$f = (3 - \partial)(\partial - 1) \frac{\rho_f \partial^2}{\mu \varepsilon_o^2 (d_p + d_s)} \left[\frac{3A}{2} + \frac{B}{4} \right] V$ $A = \frac{24 \varepsilon_o \mu}{\rho_f \partial (3 - \partial) (d_p + d_s) V}$ $B = 1 + 10 \left[\frac{(d_p + d_s) (\partial - 1) \rho_f V}{2 \mu \varepsilon_o} \right]^{-0.667}$ $\frac{\Delta P}{\Delta x} = \frac{36 \partial (\partial - 1) (3 - \partial)^2}{4 \varepsilon_o^2 d_p^2} \mu V + \frac{2.05 \partial (\partial - 1)}{2 \varepsilon_o^2 d_p} \rho V^2$
Tadrist et al. [8]	10 PPI 20 PPI 40 PPI	10 20 40	3.97 4.50 3.44	0.917 0.933 0.905	13 25 6.6	128 240 389	$\frac{\Delta P}{\Delta x} = c_1 \frac{(1 - \varepsilon_o)^2 \mu V}{\varepsilon_o^3 d_s^2} + c_2 \frac{(1 - \varepsilon_o) \rho V^2}{\varepsilon_o^3 d_s}$ $100 \leq c_1 \leq 865_1 \text{ and } 0.65 \leq c_2 \leq 2.6$
Moreira et al. [26]	Sample 1 Sample 2 Sample 3	8 20 45	2.3 0.8 0.36	0.94 0.88 0.76	23.5 8.07 0.942	322 580 1708	$\frac{\Delta P}{\Delta x} = 1.275 \times 10^9 \frac{(1 - \varepsilon_o)^2}{\varepsilon_o^3 d_p^{-0.05}} \mu V + 1.89 \times 10^4 \frac{(1 - \varepsilon_o)}{\varepsilon_o^3 d_p^{-0.25}} \rho V^2$
Topin et al. [31]	NC3743 NC2733 NC1723 NC1116	— — — —	0.569 0.831 1.84 2.45	0.87 0.91 0.88 0.89	0.213 0.444 2.81 6.02	1330 1075 490 381	$\frac{\Delta P}{\Delta x} = \frac{1}{1.391 \times 10^{-4}} \frac{(1 - \varepsilon_o)^2 \mu V}{\varepsilon_o^3 d_s^2} + 1.32 a_c \rho V^2$
Dukhan [32]	Sample 1 Sample 2 Sample 3 Sample 4 Sample 5	10 10 20 20 40	— — — — —	0.919 0.915 0.919 0.924 0.923	10 8.0 6.3 5.4 4.7	210 270 290 280 380	<p>10 PPI : $K = 10^{-8} (0.0031 e^{0.0955 \varepsilon_o})$, $C = 100 (-2.399 \varepsilon_o + 222)$</p> <p>20 PPI : $K = 10^{-8} (0.0009 e^{0.0946 \varepsilon_o})$, $C = 100 (-1.146 \varepsilon_o + 108)$</p> <p>40 PPI : $K = 10^{-8} (8 \times 10^{-7} e^{0.0955 \varepsilon_o})$, $C = 100 (-0.613 \varepsilon_o + 58)$</p>

Table 1 (continued)

References	Sample	PPI	$d_p \times 10^{-3}$ (m)	ε_o	$K \times 10^{-8}$ (m ²)	C (m ⁻¹)	Correlation for pressure drop prediction		
Mancin et al. [47]	Al-5-7.9	5	5.08	0.921	2.36	205	$\frac{\Delta P}{\Delta x} = \frac{2FG^2}{\rho d_h}$ with $G = \rho V$ and $F = \frac{1.765 \cdot \varepsilon_o^2 \cdot \text{Re}^{-0.1014}}{\text{PPI}^{0.6}}$		
	Al-10-9.7	10	2.54	0.903	19.0	170			
	Al-10-6.6	10	2.54	0.934	18.7	190			
	Al-10-4.4	10	2.54	0.956	18.2	240			
	Al-20-6.8	20	1.27	0.932	8.24	226			
	Al-40-7.0	40	0.635	0.930	6.34	342			
Inayat et al. [4]	Sample 1	—	3.085	0.871	—	—	$\text{Re} = \frac{d_h \cdot G}{\mu \cdot \varepsilon_o}$ where, $d_h = \frac{2 \left(\frac{0.0254}{\text{PPI}} - d_s \right) \cdot L}{\left(\frac{0.0254}{\text{PPI}} - d_s + L \right)}$		
	Sample 2	—	2.397	0.846	—	—			
	Sample 3	—	1.689	0.799	—	—			
Dietrich et al. [3]	Al ₂ O ₃	20	1.529	0.69	13	1204.1	$\frac{\Delta P}{\Delta x} = 110 \frac{1}{\varepsilon_t} \frac{\mu V}{d_h^2} + 1.45 \frac{1}{\varepsilon_t^2} \frac{\rho V^2}{d_h}$; $\text{Hg} = \frac{\Delta P d_h^3}{\Delta x \rho V^2}$ $\text{Hg} = 110\text{Re} + 1.45\text{Re}^2$ with $\text{Re} = \frac{\mu d_h}{\varepsilon_t \nu}$		
	Al ₂ O ₃	10	2.253	0.765	7.7	492.88			
	Al ₂ O ₃	20	1.091	0.748	5.4	939.85			
	Al ₂ O ₃	30	0.884	0.752	3.2	1122.3			
	Al ₂ O ₃	45	0.625	0.757	2.0	1257.8			
	Al ₂ O ₃	20	1.464	0.811	14.4	496.44			
	Mullite	20	1.348	—	9.0	1179.7			
	Mullite	10	2.111	—	29.9	551.12			
	Mullite	20	1.405	0.741	8.8	753.64			
	Mullite	30	1.127	0.748	4.5	836.32			
	Mullite	45	0.685	0.744	2.9	1527.3			
	Mullite	20	1.522	—	12.0	506.55			
	OBSiC	20	1.361	—	6.5	1004.6			
	OBSiC	10	2.257	—	27.0	770.22			
	OBSiC	20	1.489	—	5.6	831.72			
	OBSiC	30	1.107	—	4.6	1203.8			
	Kumar and Topin [11]	Sample 1	—	—	0.60	6		1157	$\frac{\Delta P}{\Delta x} = E_1 \frac{(1 - \varepsilon_o)^2}{\varepsilon_o^3} a_c^2 \mu V + E_2 \frac{(1 - \varepsilon_o)}{\varepsilon_o^3} a_c \rho V^2$
		Sample 2	—	—	0.65	7.4		967	
	Samples 1–8 (circular strut shape)	Sample 3	—	—	0.70	9		748	$\frac{E_1}{(1 - \varepsilon_o)^2} = \sqrt{\alpha_{\text{eq}}} \cdot \text{Exp}(4.4293n^{0.403})$
		Sample 4	—	—	0.75	11		530	
Samples 9–16 (square strut shape)	Sample 5	—	—	0.80	13.5	409	$\frac{E_2}{(1 - \varepsilon_o)^3} = \sqrt{\alpha_{\text{eq}}} \cdot \text{Exp}(1.5)n^{3.15}$		
	Sample 6	—	—	0.85	16.7	304			
	Sample 7	—	—	0.90	21.2	197			
Samples 17–20 (rotated square strut shape)	Sample 8	—	—	0.95	28.6	106	$n = \frac{\varepsilon_o}{1 - \varepsilon_o}$		
	Sample 9	—	—	0.60	3.4	2603			
	Sample 10	—	—	0.65	4.7	1663			
	Sample 11	—	—	0.70	6.3	1134			
	Sample 12	—	—	0.75	8.3	796			

Table 1 (continued)

References	Sample	PPI	$d_p \times 10^{-3}$ (m)	ε_o	$K \times 10^{-8}$ (m ²)	C (m ⁻¹)	Correlation for pressure drop prediction
Samples 21–24 (diamond strut shape)	Sample 13	—	—	0.80	10.7	570	
	Sample 14	—	—	0.85	13.9	398	
	Sample 15	—	—	0.90	18.4	234	
	Sample 16	—	—	0.95	26.2	100	
Samples 25–32 (hexagon strut shape)	Sample 17	—	—	0.80	12.4	730	
	Sample 18	—	—	0.85	15.6	557	
	Sample 19	—	—	0.90	20	347	
Samples 33–37 (star strut shape)	Sample 20	—	—	0.95	27.5	175	
	Sample 21	—	—	0.80	13.8	740	
	Sample 22	—	—	0.85	16.6	611	
	Sample 23	—	—	0.90	20.6	453	
	Sample 24	—	—	0.95	27.7	221	
	Sample 25	—	—	0.60	6	1362	
	Sample 26	—	—	0.65	7.4	1139	
	Sample 27	—	—	0.70	9.1	784	
	Sample 28	—	—	0.75	11.3	561	
	Sample 29	—	—	0.80	13.9	416	
	Sample 30	—	—	0.85	17.5	277	
	Sample 31	—	—	0.90	22.6	175	
	Sample 32	—	—	0.95	31.1	95	
	Sample 33	—	—	0.75	8.1	1502	
	Sample 34	—	—	0.80	10.9	896	
	Sample 35	—	—	0.85	14.1	603	
	Sample 36	—	—	0.90	18.7	366	
	Sample 37	—	—	0.95	27.4	152	
Kumar and Topin [12]	Sample 1	—	—	0.80	96.9	391.9	$\frac{\Delta P}{\Delta x} = E_1 \frac{(1 - \varepsilon_o)^2}{\varepsilon_o^3} a_c^2 \mu V + E_2 \frac{(1 - \varepsilon_o)}{\varepsilon_o^3} a_c \rho V^2$ $E_1 = 6.5373 \frac{\varepsilon_o}{(1 - \varepsilon_o)^2} \sqrt{\frac{\beta}{\alpha}}; E_2 = 2.9314 \varepsilon_o^2 \sqrt{\frac{\beta}{\alpha}}$
	Sample 2	—	—	0.85	140	191.9	
	Sample 3	—	—	0.90	199	100.7	
	Sample 4	—	—	0.95	309	40.8	
Kumar and Topin [13]	Al ₂ O ₃	20	1.529	0.69	13	1204.1	$\frac{\Delta P}{\Delta x} = E_1 \frac{(1 - \varepsilon_o)^2}{\varepsilon_o^3} a_c^2 \mu V + E_2 \frac{(1 - \varepsilon_o)}{\varepsilon_o^3} a_c \rho V^2$ $E_1 = \frac{\varepsilon_t \cdot d_h^2}{K_D} \cdot \varepsilon_o (\alpha/\beta)^{-1}; E_2 = C_{For} \cdot \varepsilon_t^2 \cdot d_h \cdot \varepsilon_o (\alpha/\beta)^{-1}$ $d_h = \frac{4\varepsilon_t}{a_c}$
	Al ₂ O ₃	10	2.253	0.765	7.7	492.88	
	Al ₂ O ₃	20	1.091	0.748	5.4	939.85	
	Al ₂ O ₃	30	0.884	0.752	3.2	1122.3	
	Al ₂ O ₃	45	0.625	0.757	2.0	1257.8	
	Al ₂ O ₃	20	1.464	0.811	14.4	496.44	
	Mullite	20	1.348	—	9.0	1179.7	
	Mullite	10	2.111	—	29.9	551.12	
	Mullite	20	1.405	0.741	8.8	753.64	
	Mullite	30	1.127	0.748	4.5	836.32	
	Mullite	45	0.685	0.744	2.9	1527.3	
	Mullite	20	1.522	—	12.0	506.55	
	OBSiC	20	1.361	—	6.5	1004.6	
	OBSiC	10	2.257	—	27.0	770.22	
	OBSiC	20	1.489	—	5.6	831.72	
	OBSiC	30	1.107	—	4.6	1203.8	

presented friction factor and calculated Reynolds number based on square root of Forchheimer permeability ($Re = \rho V \sqrt{K_{For}/\mu}$). Though their samples were of very high porosity (0.90–0.93), the dispersion in the friction factor is quite significant. Comparison between predicted and experimental pressure drop data has been discussed only in inertia regime (at high Re).

Dietrich et al. [3] proposed a pressure drop correlation (establishing $Hg - Re$ relationship) based on a slightly modified Ergun-like equation and was adapted to the experimental values only by using the hydraulic diameter (d_h) based on the specific surface area (a_c) and the total porosity (ϵ_t). The authors obtained numerical constants of 110 and 1.45 for Ergun parameters E_1 and E_2 , respectively, for ceramic foams of 10, 20, 30, and 45 PPI. However, it should be noted that the correlation presented between d_h and PPI was served as additional information and was not used for correlating the experimental values and the development of the pressure drop correlation. Dietrich [5] applied the correlation of Dietrich et al. [3] to numerous data sets for ceramic and metal foams from the literature. The correlation predicted these data to be within 40% margin of error in a wide porosity range ($0.70 < \epsilon_o < 0.98$).

In the case of open-cell foam samples of a given pore size and for a wide range of porosity ($0.60 < \epsilon_o < 0.85$), inertia coefficient varies tremendously and depends strongly on strut shape. With respect to strut shapes of either metal or ceramic foams, Ergun parameters cannot have constant numerical values, but they are strict functions of foam geometry [4,11–13,23,50,59].

Inayat et al. [4] developed a dimensionless correlation of Ergun parameters, E_1 and E_2 ; those depend upon the window diameter, strut diameter, and open porosity of the foams. The authors argued that the numerical values appearing in their correlations are geometric constants of foam geometry. Their correlations showed that the Ergun-like equation with fixed parameters or constant coefficients (E_1 and E_2) cannot be applied to predict pressure drop for foam structures in the wide range of porosity $0.70 < \epsilon_o < 0.85$. Kumar and Topin [11] derived correlations to predict E_1 and E_2 from CFD numerical pressure drop data on virtual foam samples with different strut shapes. Their foams were of approximately identical pore size with porosity in the range, $0.60 < \epsilon_o < 0.95$. The authors tried to encapsulate the impact of different strut shapes with the characteristic size of strut cross section and an averaged value of exponent on the porosity function appeared in their correlation (see Table 1). Their calculated pressure drop data were in good agreement with the CFD numerical pressure drop data. However, these authors [4,11] did not present the validation of flow law characteristics separately in Darcy and inertia regimes.

In the literature, most of the authors have compared and validated the values calculated from pressure drop data correlations against experimental and CFD numerical pressure drop data. Most of the experimental flow law characteristics data were obtained within a moderate to high Reynolds number range ($Re > 10$). Thus, K_{For} values have been mostly reported in the literature. However, K_{For} is different for same type of foams depending upon the velocity range and does not represent permeability in a Darcy regime. Moreover, inertia coefficient is dominant in the studied range of velocity and usually nullifies the effect of the viscous regime when comparing and validating the pressure drop data from the correlations.

Kumar and Topin [12] presented the pressure drop correlations for an equilateral triangular strut and related the Ergun parameters with the characteristic strut size and length for the porosity range of $0.80 < \epsilon_o < 0.95$. The authors validated the calculated and measured pressure drop data separately in Darcy and inertia regimes. They argued that working on the whole range of flow rate masks the errors mainly for the Darcy regime and does not allow for a correct evaluation of the prediction quality. Kumar and Topin [13] derived the correlations for ceramic foams and modified the pressure drop correlation presented by Dietrich et al. [3]. The authors [13] have introduced a dimensionless factor to

correct the Ergun parameters derived by Dietrich et al. [3] and showed that the correlation provides good estimates of flow law characteristics when the correct values of open porosity (ϵ_o) and geometrical parameters are considered.

After a careful analysis of different correlations and large dispersion of data, it can be highlighted that:

- Published values of K_{For} are actually velocity range dependent and vary according to data extraction methods.
- No individual validations are carried out according to the flow regimes.
- Incompatible use of constant or variable values of Ergun coefficients.
- Applicability of any given correlation to a given foam sample cannot be guaranteed.

From the previous paragraphs, it is very clear that no generally applicable correlation for the pressure drop prediction in the open cell foams has yet been proposed. Therefore, further work is definitely needed in this area. Moreover, very few data of flow law characteristics in Darcy and inertia regimes (K_D and C_{For}) are reported in the literature [9,11,12] in a wide porosity range. It is, thus, imperative to examine the validity and applicability of pressure drop correlations in these regimes.

3 Performance of the State-of-the-Art of Pressure Drop Correlations

This section is divided into two subsections, i.e., comparison of calculated and measured pressure drop data in the entire velocity range (viscous and inertia regimes) and comparison of flow law characteristics (K_D and C_{For}) for different strut shapes and for the whole accessible porosity range ($0.60 < \epsilon_o < 0.95$). Based on the analysis presented in Sec. 2 about the inconsistencies in pressure drop values from experiments, we chose to show the comparison between CFD numerical values of pressure drop values reported in the works of Kumar and Topin [11,12] due to four main reasons: (1) pressure drop values were not biased along the foam length, (2) permeability obtained in Darcy regime, (3) pressure drop values strictly follow Forchheimer equation, and (4) availability of virtual foam samples based on Kelvin-like cell structure of different strut cross sections.

3.1 Comparison Between Calculated and Measured Pressure Drop Data. Based on the numerical flow law characteristics, i.e., the Darcian permeability (K_D) and the Forchheimer inertia coefficient (C_{For}) reported in the works of Kumar and Topin [11,12], flow law characteristics obtained for equilateral triangular and circular strut cross sections have been compared against the correlations presented in the literature. The reason to choose these two shapes for comparison is to investigate the influence of strut shapes on flow law characteristics and also due to the fact that various authors have reported a change in the strut shape from circular to convex or concave or equilateral triangular from low to high porosity (see also Inayat et al. [4], Bhattacharya et al. [25]).

The measured pressure drop data reported in the works of Kumar and Topin [11,12] are mainly compared against the correlations presented by Dietrich et al. [3], Inayat et al. [4], Lacroix et al. [20], Moreira et al. [26], Khayargoli et al. [28], and Liu et al. [30] and are presented in Figs. 2 and 3 for equilateral triangular and circular strut cross sections, respectively. These correlations [3,4,20,26,28,30] were chosen based on the Ergun parameters and the different types of morphological parameters employed. In order to compare the calculated pressure drop data [11,12] with the predicted values from the correlations, pseudo experimental velocity values (very low velocity to determine viscous condition and high velocity to determine inertia condition; $10^{-7} \leq V \leq 10^3$) and an arbitrary fluid ($\rho = 0.8887 \text{ kg m}^{-3}$; $\mu = 998.5 \text{ kg m}^{-3}$) were chosen. The general observation suggests that none of the

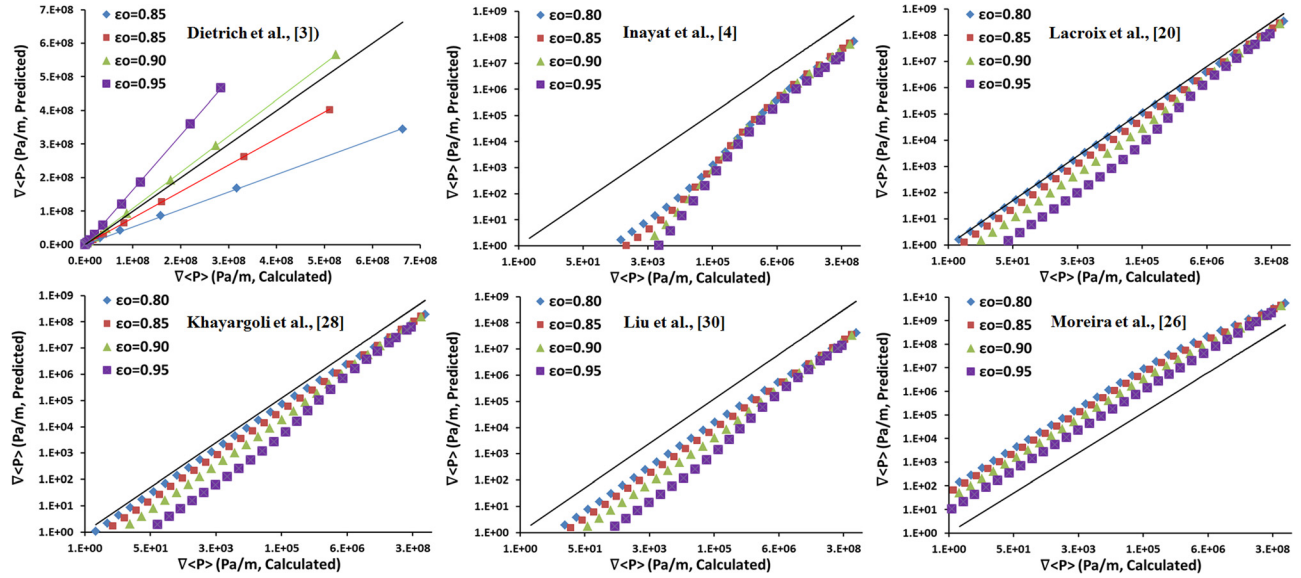


Fig. 2 Performance of state-of-the-art correlations (black line corresponds to the measured numerical data Kumar and Topin [12]). The comparison presented earlier is performed for equilateral triangular strut shape.

correlations from the open literature could reproduce the numerical pressure drop values to a satisfactory level (see Figs. 2 and 3).

3.1.1 In the Case of Equilateral Triangular Strut Shape. The predicted values of pressure drop using the correlation of Dietrich et al. [3] are underestimated and overestimated by a factor of 1.5–1.6 (error ~ 150 – 160%) compared to the calculated pressure drop data in the porosity range, $0.80 < \varepsilon_o < 0.95$. Moreover, for the porosity, $\varepsilon_o = 0.90$, the error between predicted and calculated pressure drop values is 10%.

When compared the calculated pressure drop values against the correlation established by Inayat et al. [4], the error is quite significant. The predicted values for all porosities are underestimated by a factor of 200–20,000 in Darcy regime, while it varies by a factor of 10–1400 in the inertia regime.

The predicted values of pressure drop from the correlation of Lacroix et al. [20] and Khayargoli et al. [28] are underestimated compared to calculated values of pressure drop. The error is varying between 80% and 100% in Darcy and inertia regimes from low to high porosity. The Ergun parameters in the formulation of these authors are very close, and thus, their correlations provide almost the same order of results. The errors are more significant with increasing porosity.

Pressure drop values predicted from the correlation of Liu et al. [30] underestimates the calculated values and the error is varying between 700% and 17,000% in Darcy regime while 1000–5000% in inertia regime.

Pressure drop values predicted from the correlation of Moreira et al. [26] are overestimated in the entire range of porosity. The error estimated between predicted and calculated values is 18–2500% in the Darcy regime, while it is 80–200% in the inertia regime from low to high porosity. The error increases with decreasing porosity.

3.1.2 In the Case of Circular Strut Shape. The predicted values of pressure drop of the circular strut shape by using the correlation of Dietrich et al. [3] are overestimated. The error is 140–165% in both regimes for low porosity ($\varepsilon_o = 0.60$) and increases with porosity.

The correlations of Inayat et al. [4] lead to the errors in the predicted pressure drop values in the Darcy and inertia regimes of more than 1000–2500% and 100–4000%, respectively.

The correlation of Lacroix et al. [20] results in an overestimation (respectively, underestimation) of predicted pressure drop values in the porosity range $0.60 < \varepsilon_o < 0.85$ (respectively, 0.90

$< \varepsilon_o < 0.95$). The error ranges are 84–3000% and 60–400% in Darcy and inertia regimes. However, in the porosity range $0.85 < \varepsilon_o < 0.90$, the correlation provides a good estimate in inertia regime (error range ~ 10 – 30%), while the error in the Darcy regime is 70–300%.

Similar trend of underestimating and overestimating the calculated pressure drop values is observed for the correlation by Khayargoli et al. [28]. However, the error is quite significant compared to the correlation of Lacroix et al. [20]. The error lies in the range of 70–4500% and 40–600%, respectively, in the Darcy and inertia regimes.

The correlation of Liu et al. [30] underestimates the calculated values of pressure drop by a factor of 2–200 (error ~ 20 – $20,000\%$) same as the case of equilateral triangular strut shape.

The correlation of Moreira et al. [26] overestimates the pressure drop data. The errors in the porosity range, $0.60 < \varepsilon_o < 0.90$, are significant. The error in pressure drop values is least, varying between 30% and 60% for 90% porosity only.

No correlation compares well with pore scale numerical pressure drop data and predicts entirely different results according to (1) porosity range and (2) strut shape. Although each of these correlations gives good results against their original experimental (respectively, numerical) data that have been used to derive them, but none of these correlations could be applied to an arbitrary chosen set of pressure drop data and foam samples.

From the previous comparisons presented in Figs. 2 and 3, it is, thus, evident that strut shape plays an important role in determining flow law characteristics of open-cell foams and for a wide porosity range ($0.60 < \varepsilon_o < 0.95$). Moreover, Ergun parameters do not possess constant numerical values, but they are strictly functions of the geometrical parameters of the foam geometry. Thus, it can be concluded that none of the correlations reported in the literature bears a general applicability.

3.2 Comparison of Fluid Flow Law Characteristics.

Kumar and Topin [11] presented a pressure drop correlation based on Ergun-like approach for different strut shapes of virtual foam samples by averaging the exponent appearing in the porosity function. Their correlation contains a dimensionless geometrical parameter which suggests that the Ergun parameters do not have constant numerical values. The Darcian permeability and Forchheimer inertia coefficient for different strut shapes are predicted using their correlation and are presented in Fig. 4 (left and right)

for the porosity range of $0.60 < \varepsilon_o < 0.95$. The predicted values of Darcian permeability are scattered and the correlation leads to scattered K_D values compared to the numerical ones (see Fig. 4, left), which implies that the comparison of predicted and numerically calculated values of pressure drop leads to inaccurate results in Darcy regime. These inaccuracies actually do not get detected due to the impact of high inertia effect in the entire velocity range. On the other hand, Forchheimer inertia coefficients compare well with the correlation except for complex strut shapes (e.g., square, diamond, and star) at low porosity only (see Fig. 4, right). At low porosity ($0.60 < \varepsilon_o < 0.80$), the averaged value of exponent in the porosity function and the approximated dimensionless geometrical parameters lead to a slight loss of accuracy.

This comparison (Fig. 4) suggests that it is very difficult to obtain the precise values of flow law characteristics for an arbitrary strut shape using an averaged value of the exponents in the porosity function. Thus, systematic studies need to be carried out to obtain the exponents and constants in the correlations for different strut shapes using an Ergun-like approach in order to achieve high precision in predicting pressure drop data. On the other hand, for most of the commercially available foams, the averaged value would be sufficient, as strut shape (from circular to triangle strut shape) does not vary much in high porosity range.

Kumar and Topin [12] presented a correlation to predict Ergun parameters but limited to equilateral triangular strut shape only. The authors derived the correlations by taking into account Darcy and inertia regimes simultaneously and related Ergun parameters with dimensionless geometrical parameters and porosity, respectively. The comparison of their correlation with the pressure drop data and flow law characteristics reported in the literature is presented in Table 2 for the foam samples that present a nearly equilateral triangular strut cross section. The results of E_2 and, subsequently, C_{For} are validated very well. On the other hand, K_D cannot be compared with K_{For} and the values of K_D are lower than K_{For} by approximately two order of magnitude for all the samples (see Table 2).

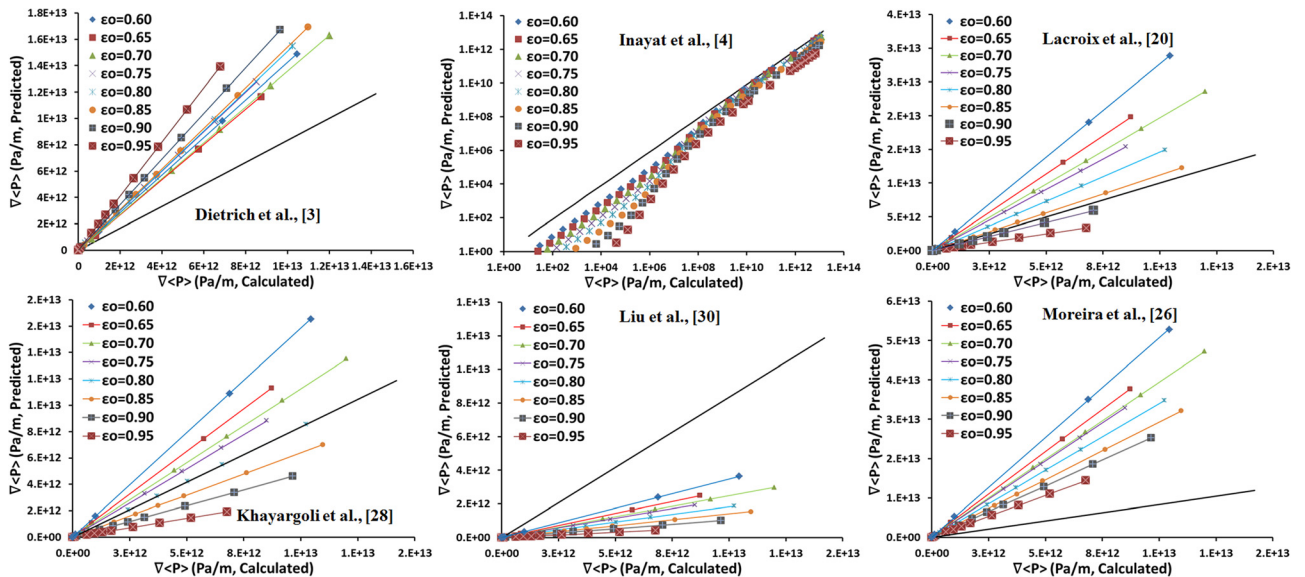
4 Remarks on Nonapplicability of Correlations

We examined and compared various correlations with respect to the pore scale numerical pressure drop data for equilateral triangular and circular strut cross sections. From the comparison, it is evident that the errors or discrepancies in pressure drop data are based on several critical parameters as follows:

- Correlations which are based on data obtained from high-porosity foam samples and geometrical parameters do not play a significant role for such foam samples.
- The use of simplified foam geometry leads to ill-estimation of specific surface area.
- Extraction of K_{For} instead of K_D .
- Simultaneous measurements of permeability and inertia coefficient in an arbitrary Re range using polynomial fit of pressure drop data.
- Global validation of measured pressure drop data over the entire velocity range.
- No separate validation of flow law characteristics, i.e., permeability and inertia coefficient.
- Choice of characteristic length scale.

From Figs. 2 and 3, the correlation proposed by Dietrich et al. [3] exhibits the lowest error for the two strut shapes (equilateral triangular and circular strut shapes) presented in this work, while the other correlations exhibit large errors and fall out of the range compared with calculated pressure drop values. The comparison of these two different strut shapes clearly indicates that the Ergun parameters cannot have constant numerical values as the strut shape does play an important role in the characterization of flow properties (see Figs. 2 and 3, Inayat et al. [4], Kumar and Topin [11–13]). In the case of high porosity ($0.80 < \varepsilon_o < 0.95$), the error between calculated and measured pressure drop is less, but in the case of low porosity ($0.60 < \varepsilon_o < 0.80$), specific surface area and strut shape start to impact strongly the pressure drop values. Thus, a geometrical parameter needs to be added to the classical Ergun-like equation as presented by Kumar and Topin [11,12].

Many authors have compared calculated and measured/numerically calculated pressure drop values (e.g., see Inayat et al. [4], Dietrich [5], Kumar and Topin [11], Mancin et al. [47]) globally over the entire velocity range, which, in turn, leads to the prediction of wrong values of pressure drop in the Darcy regime that are usually neglected due to strong presence of inertia effect. On the other hand, Kumar and Topin [12] compared flow law characteristics (K_D and C_{For}) separately. Their correlation predicts excellent calculated values of the Forchheimer inertia coefficient in comparison to the literature data. The authors showed that the differences between K_D and K_{For} are indifferent in the case of high-porosity foam samples, where the experimental error in K_{For} is bigger than the error in C_{poly} . When comparing the measured pressure drop values with the experimental/numerical data for the



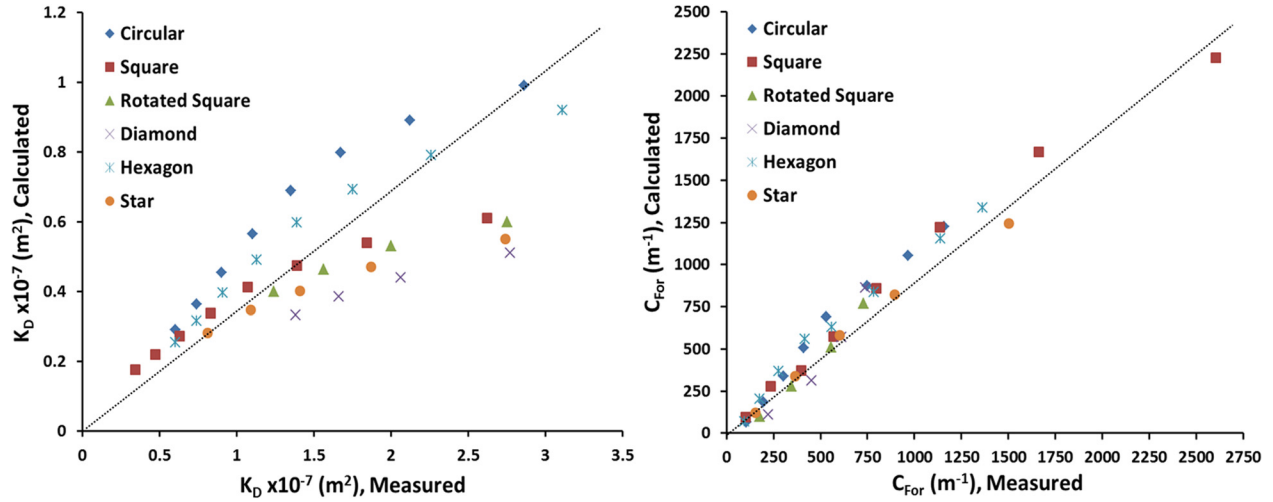


Fig. 4 Performance of state-of-the-art correlations of different strut shapes. Measured flow characteristics (K_D and C_{For}) are taken from Kumar and Topin [11].

whole velocity range, the pressure drop is mostly governed by the inertia regime (where inertia coefficient obtained is sufficient accuracy) and, thus, hides the error in permeability. This is one of the reasons that correlations in the literature are applicable to a very few foam samples of very high porosity and for a given strut shape.

It is, thus, important to validate the pressure drop values in both regimes, i.e., viscous and inertia regime separately (see Kumar and Topin [12,13]). In other words, one must compare the measured and calculated permeability and inertia coefficients in both flow regimes in order to improve the quality of the correlation that could help in reducing the dispersion in the pressure drop data (or friction factor data).

5 Conclusion

Traditionally, foams are created by processes that lead to a highly nonuniform structure with significant dispersion in size, shape, thickness, connectivity, and topology of its constituent cells. These foam structures mostly revealed circular or nearly triangular strut shapes in high-porosity foam samples. Most commonly, the correlations derived by the authors were based on the Ergun-like approach by relating easily accessible and measurable morphological parameters to flow law characteristics.

In this work, a comprehensive study has been conducted to identify bias in pressure drop data obtained experimentally, different methodologies to extract flow law characteristics from

Table 2 Validation of experimental and calculated using correlation of Kumar and Topin [12] for equilateral triangular strut cross section

Authors	Morphological data			Experimental data				Calculated data			
	Sample	ε_o	a_c (m ⁻¹)	K_{For} ($\times 10^{-7}$ m ²)	C_{poly} (m ⁻¹)	E_1	E_2	K_D ($\times 10^{-7}$ m ²)	C_{For} (m ⁻¹)	E_1	E_2
Bhattacharya et al. [25]	5 PPI	0.973	516	2.7	186.68	474.58	12.34	0.058	177.86	21,981	11.76
	5 PPI	0.912	623	1.8	200.35	123.38	2.77	0.194	190.81	1142	2.64
	10 PPI	0.949	843	1.2	280.01	196.51	5.57	0.053	266.61	4486	5.3
	10 PPI	0.914	716	1.1	211.06	157.44	2.62	0.143	200.80	1210	2.49
	20 PPI	0.955	934	1.3	257.94	170.67	5.35	0.036	245.62	6135	5.09
	20 PPI	0.925	898	1.1	313.57	118.96	3.68	0.077	298.69	1707	3.51
	40 PPI	0.927	1274	0.61	360.35	110.22	3.09	0.037	343.24	1827	2.94
	40 PPI	0.913	1308	0.53	364.87	96.47	2.44	0.044	346.90	1175	2.32
	5 PPI	0.946	689	2.17	212.52	152.19	4.84	0.085	202.60	3889	4.61
	5 PPI	0.905	636	1.74	186.99	110.86	2.29	0.205	177.70	941	2.18
	20 PPI	0.949	975	1.185	290.5	148.77	4.99	0.039	276.94	4486	4.76
	40 PPI	0.952	1300	0.562	411.7	189.25	5.69	0.020	391.99	5221	5.42
	40 PPI	0.937	1227	0.568	377.21	152.70	4.01	0.033	358.95	2643	3.82
	Boomsma et al. [49]	10 PPI	0.921	820	3.529	120	41.67	1.45	0.098	114.43	1498
20 PPI		0.92	1700	1.089	239	30.93	1.37	0.023	227.05	1451	1.3
40 PPI		0.928	2700	0.712	362	21.38	1.49	0.008	345.41	1891	1.42
Dukhan [32]	10 PPI	0.919	790	1	210	153.53	2.55	0.109	200.34	1407	2.43
	10 PPI	0.915	810	0.8	270	171.71	3.00	0.110	257.04	1246	2.86
	20 PPI	0.919	1300	0.63	290	90.00	2.14	0.040	276.77	1407	2.04
	20 PPI	0.924	1200	0.54	280	133.49	2.42	0.044	267.05	1651	2.31
	40 PPI	0.923	1800	0.47	380	67.06	2.16	0.020	361.34	1598	2.05
Mancin et al. [47]	5 PPI	0.921	339	2.36	205	364.62	5.98	0.574	195.40	1498	5.7
	10 PPI	0.934	692	1.87	190	137.86	3.39	0.110	181.06	2353	3.23
	10 PPI	0.956	537	1.82	240	378.36	8.87	0.106	228.51	6489	8.45
	20 PPI	0.932	1156	0.824	226	108.12	2.33	0.041	215.56	2183	2.22
	40 PPI	0.93	1679	0.634	342	64.29	2.34	0.020	325.84	2030	2.23

pressure drop data, the choice of the characteristic length scale, and the adaptability of empirical correlations reported in the literature. It is found that most of studies reported Forchheimer permeability. Nevertheless, it has been shown that only inertia coefficient is measured correctly. On the other hand, very few studies analyzed the permeability in viscous regime, i.e., Darcian permeability analysis. The applicability and adaptability of different correlations were tested in the wide porosity range ($0.60 < \varepsilon_o < 0.95$) for a wide range of Reynolds number.

Comparison of predicted pressure drop data showed that the correlations proposed by Dietrich [5] and Kumar and Topin [11] are in good agreement with experimental data over the whole velocity range. However, their correlations do not predict correctly the permeability in the viscous regime. The correlation proposed by Kumar and Topin [12] seems to be more adapted to estimate the pressure drop within foam structure of equilateral triangular strut shape. The predicted values of flow characteristics were validated against experimental data from many authors.

Among all the pressure drop studies and correlations presented in this review work, critical remarks are highlighted in the following:

- The permeability and inertia coefficients are very sensitive to the porosity range (mainly low-porosity range) and are strictly shape dependent.
- Separate determination of flow law characteristics (K_D and C_{For} in viscous and inertia regimes) is needed. Extraction of permeability from second-order polynomial pressure drop data would lead to wrong values of permeability in the viscous regime.
- Values of Ergun parameters vary clearly with porosity and strut shape and do not possess constant numerical values.
- Common definition of characteristic length scale (and associated measurements) is missing to reduce the dispersion in friction factor data.

Based on the aforementioned remarks, it is crucial to adapt common definitions and measurement methods to determine flow law characteristics as well as morphological parameters of foam structure. Moreover, it has also been observed that open-cell foams of the same pore diameter exhibit different flow law characteristics that depend on strut shape [11]. It is, thus, important to derive new correlations taking together viscous and inertia regimes into account that could encompass different morphological parameters on a common basis and could also be valid for different sets of foam structures having different strut cross sections in a wide range of Reynolds number.

Acknowledgment

The authors would like to thank the ANR (Agence Nationale de la Recherche) for financial support in the framework of FOAM project and all project partners for their assistance.

Nomenclature

- a_c = specific surface area (m^{-1})
 C_{For} = Forchheimer inertia coefficient (Eq. (2)) (m^{-1})
 C_L = characteristic length scale (mm)
 C/C_{poly} = inertia coefficient obtained using polynomial curve (m^{-1})
 d_h = hydraulic diameter (mm)
 d_p = pore diameter (mm)
 d_s = strut diameter (mm)
 D_p = equivalent particle diameter (mm)
 E_1 = Ergun parameter of viscous component (Eq. (4))
 E_2 = Ergun parameter of inertia component (Eq. (4))
 f = friction factor
 Hg = Hagen number
 K_D = Darcian permeability (Eq. (1)) (m^2)

K/K_{For} = Forchheimer permeability/ permeability obtained using polynomial curve (m^2)

Re = Reynolds number

V = superficial fluid velocity ($m\ s^{-1}$)

$\Delta P/\Delta x$ = pressure drop per unit length ($Pa\ m^{-1}$)

Greek Symbols

α_{eq} = ratio of strut diameter (or side length of strut shape) to node to node length

β = ratio of strut length to node to node length

γ = dimensionless cubic law parameter (Eq. (3))

ε_o = open porosity

ε_t = total porosity

μ = dynamic fluid viscosity ($Pa \cdot s$)

ρ = fluid density ($kg\ m^{-3}$)

∂ = tortuosity (Table 1)

References

- [1] Dukhan, N., 2012, *Metal Foam: Fundamentals and Applications*, DESTech, Lancaster, PA.
- [2] Garrido, G. I., Pateas, F. C., Lang, S., and Kraushaar-Czarnetzki, B., 2008, "Mass Transfer and Pressure Drop in Ceramic Foams: A Description of Different Pore Sizes and Porosities," *Chem. Eng. Sci.*, **63**(21), pp. 5202–5217.
- [3] Dietrich, B., Schabel, W., Kind, M., and Martin, H., 2009, "Pressure Drop Measurements of Ceramic Sponges-Determining the Hydraulic Diameter," *Chem. Eng. Sci.*, **64**(16), pp. 3633–3640.
- [4] Inayat, A., Schwerdtfeger, J., Freund, H., Korner, C., Singer, R. F., and Schwieger, W., 2011, "Periodic Open-Cell Foams: Pressure Drop Measurements and Modeling of an Ideal Tetraikadecahedra Packing," *Chem. Eng. Sci.*, **66**(12), pp. 2758–2763.
- [5] Dietrich, B., 2012, "Pressure Drop Correlation for Ceramic and Metal Sponges," *Chem. Eng. Sci.*, **74**, pp. 192–199.
- [6] Gibson, L. J., and Ashby, M. F., 1997, *Cellular Solids: Structure and Properties*, 2nd ed., Cambridge University Press, Cambridge, UK.
- [7] Banhart, J., 2001, "Manufacture, Characterization and Application of Cellular Metals and Metal Foams," *Prog. Mater. Sci.*, **46**(6), pp. 559–632.
- [8] Tadrast, L., Miscevic, M., Rahli, O., and Topin, F., 2004, "About the Use of Fibrous Materials in Compact Heat Exchangers," *Exp. Therm. Fluid Sci.*, **28**(2–3), pp. 193–199.
- [9] Dukhan, N., and Minjeur, C., 2011, "A Two-Permeability Approach for Assessing Flow Properties in Metal Foam," *J. Porous Mater.*, **18**(4), pp. 417–424.
- [10] De Jaeger, P., T'Joens, C., Huisseune, H., Ameel, B., De Schampheleire, S., and De Paep, M., 2013, "Influence of Geometrical Parameters of Open-Cell Aluminum Foam on Thermohydraulic Performance," *Heat Transfer Eng.*, **34**(14), pp. 1202–1215.
- [11] Kumar, P., and Topin, F., 2014, "Micro-Structural Impact of Different Strut Shapes and Porosity on Hydraulic Properties of Kelvin Like Metal Foams," *Transp. Porous Media*, **105**(1), pp. 57–81.
- [12] Kumar, P., and Topin, F., 2014, "Investigation of Fluid Flow Properties in Open-Cell Foams: Darcy and Weak Inertia Regimes," *Chem. Eng. Sci.*, **116**(6), pp. 793–805.
- [13] Kumar, P., and Topin, F., 2014, "The Geometric and Thermo-Hydraulic Characterization of Ceramic Foams: An Analytical Approach," *Acta Mater.*, **75**, pp. 273–286.
- [14] Mahjoob, S., and Vafai, K., 2008, "A Synthesis of Fluid and Thermal Transport Models for Metal Foam Heat Exchangers," *Int. J. Heat Mass Transfer*, **51**(15–16), pp. 3701–3711.
- [15] Boomsma, K., and Poulikakos, D., 2002, "The Effects of Compression and Pore Size Variations on the Liquid Flow Characteristics in Metal Foams," *ASME J. Fluids Eng.*, **124**(1), pp. 263–272.
- [16] Bonnet, J. P., Topin, F., and Tadrast, L., 2008, "Flow Laws in Metal Foams: Compressibility and Pore Size Effects," *Transp. Porous Media*, **73**(2), pp. 233–254.
- [17] Mei, C. C., and Auriault, J. L., 1991, "The Effect of Weak Inertia on Flow Through a Porous Medium," *J. Fluid Mech.*, **222**, pp. 647–663.
- [18] Wodie, J. C., and Levy, T., 1991, "Correction non linéaire de la loi de Darcy," *C. R. Acad. Sci.*, **312**(2), pp. 157–161.
- [19] Ergun, S., and Orning, A. A., 1949, "Fluid Flow Through Randomly Packed Columns and Fluidized Beds," *Ind. Eng. Chem.*, **41**(6), pp. 1179–1184.
- [20] Lacroix, M., Nguyen, P., Schweich, D., Huu, C. P., Savin-Poncet, S., and Edouard, D., 2007, "Pressure Drop Measurements and Modeling on SiC Foams," *Chem. Eng. Sci.*, **62**(12), pp. 3259–3267.
- [21] Lu, T. J., Stone, H. A., and Ashby, M. F., 1998, "Heat Transfer in Open-Cell Metal Foams," *Acta Mater.*, **46**(10), pp. 3619–3635.
- [22] Innocentini, M. D. M., Salvini, V. R., Coury, J. R., and Pandolfelli, V. C., 1999, "Prediction of Ceramic Foams Permeability Using Ergun's Equation," *J. Mater. Res.*, **4**(4), pp. 283–289.
- [23] Richardson, J. T., Peng, Y., and Remue, D., 2000, "Properties of Ceramic Foam Catalyst Supports: Pressure Drop," *Appl. Catal. A*, **204**(1), pp. 19–32.
- [24] Fourie, J. G., and Du Plessis, P., 2002, "Pressure Drop Modelling in Cellular Metallic Foams," *Chem. Eng. Sci.*, **57**(14), pp. 2781–2789.

- [25] Bhattacharya, A., Calmidi, V. V., and Mahajan, R. L., 2002, "Thermophysical Properties of High Porosity Metal Foams," *Int. J. Heat Mass Transfer*, **45**(5), pp. 1017–1031.
- [26] Moreira, E. A., Innocentini, M. D. M., and Coury, J. R., 2004, "Permeability of Ceramic Foams to Compressible and Incompressible Flow," *J. Eur. Ceram. Soc.*, **24**(10–11), pp. 3209–3218.
- [27] Moreira, E. A., and Coury, J. R., 2004, "The Influence of Structural Parameters on the Permeability of Ceramic Foams," *Braz. J. Chem. Eng.*, **21**(1), pp. 23–33.
- [28] Khayargoli, P., Loya, V., Lefebvre, L. P., and Medraj, M., 2004, "The Impact of Microstructure on the Permeability of Metal Foams," The Canadian Society for Mechanical Engineering, Ottawa, ON, Canada.
- [29] Giani, L., Groppi, G., and Tronconi, E., 2005, "Mass-Transfer Characterization of Metallic Foams as Supports for Structured Catalysts," *Ind. Eng. Chem. Res.*, **44**(14), pp. 4993–5002.
- [30] Liu, J. F., Wu, W. T., Chiu, W. C., and Hsieh, H., 2006, "Measurement and Correlation of Friction Characteristic of Flow Through Foam Matrixes," *Exp. Therm. Fluid Sci.*, **30**(4), pp. 329–336.
- [31] Topin, F., Bonnet, J. P., Madani, B., and Tadrist, L., 2006, "Experimental Analysis of Multiphase Flow in Metallic Foam: Convective Boiling, Flow Laws and Heat Transfer," *Adv. Mater. Eng.*, **8**(9), pp. 890–899.
- [32] Dukhan, N., 2006, "Correlations for the Pressure Drop for Flow Through Metal Foam," *Exp. Fluids*, **41**(4), pp. 665–672.
- [33] Huu, T. T., Lacroix, M., Huu, C. P., Schweich, D., and Edouard, D., 2009, "Towards a More Realistic Modeling of Solid Foam: Use of the Pentagonal Dodecahedron Geometry," *Chem. Eng. Sci.*, **64**(24), pp. 5131–5142.
- [34] Brun, E., 2009, "3D Imaging of the Structures to Study the Transport Mechanisms in Cellular Medium," Ph.D. thesis, University of Aix-Marseille, Marseille, France.
- [35] Haussener, S., Coray, P., Lipinski, W., Wyss, P., and Steinfeld, A., 2010, "Tomography-Based Heat and Mass Transfer Characterization of Reticulate Porous Ceramics for High-Temperature Processing," *ASME J. Heat Transfer*, **132**(2), pp. 23305–23309.
- [36] Lawrence, H., Zhang, L. C., Dean, T., and Edmond, L., 2010, "Measurement of Tortuosity in Aluminum Foams Using Airborne Ultrasound," *Ultrasonics*, **50**(1), pp. 1–5.
- [37] Kumar, P., Topin, F., and Vicente, J., 2014, "Determination of Effective Thermal Conductivity From Geometrical Properties: Application to Open-Cell Foams," *Int. J. Therm. Sci.*, **81**, pp. 13–28.
- [38] Bastawros, A. F., Evans, A. G., and Stone, H. A., 1998, "Evaluation of Cellular Metal Heat Transfer Media," Harvard University, Cambridge, MA, Report No. MECH 325.
- [39] Lage, J. L., Antohe, B. V., and Nield, D. A., 1997, "Two Types of Nonlinear Pressure-Drop Versus Flow-Rate Relation Observed for Saturated Porous Media," *ASME J. Fluid Eng.*, **119**(3), pp. 700–706.
- [40] Bastawros, A. F., 1998, "Effectiveness of Open-Cell Metallic Foams for High Power Electronic Cooling," Symposium on the Thermal Management of Electronics, Anaheim, CA.
- [41] Hwang, J. J., Hwang, G. J., Yeh, R. H., and Chao, C. H., 2002, "Measurement of Interstitial Convective Heat Transfer and Frictional Drag for Flow Across Metal Foams," *ASME J. Heat Transfer*, **124**(1), pp. 120–129.
- [42] Seguin, D., Montillet, A., and Comiti, J., 1998, "Experimental Characterization of Flow Regimes in Various Porous Media—I: Limit of Laminar Flow Regime," *Chem. Eng. Sci.*, **53**(21), pp. 3751–3761.
- [43] Paek, J. W., Kang, B. H., Kim, S. Y., and Hyun, J. M., 2000, "Effective Thermal Conductivity and Permeability of Aluminium Foam Materials," *Int. J. Thermophys.*, **21**(2), pp. 453–464.
- [44] Kim, S. Y., Paek, J. W., and Kang, B. H., 2000, "Flow and Heat Transfer Correlations for Porous Fin in a Plate-Fin Heat Exchanger," *ASME J. Heat Transfer*, **122**(3), pp. 572–578.
- [45] Crosnier, S., Rivam, R., Bador, B., and Blet, V., 2003, "Modeling of Gas Flow Through Metallic Foams," First European Hydrogen Energy Conference (EHEC), Grenoble, France, Sept. 2–5.
- [46] Dukhan, N., and Patel, P., 2008, "Equivalent Particle Diameter and Length Scale for Pressure Drop in Porous Metals," *Exp. Therm. Fluid Sci.*, **32**(5), pp. 1059–1067.
- [47] Mancin, S., Zilio, C., Cavallini, A., and Rossetto, L., 2010, "Pressure Drop During Air Flow in Aluminum Foams," *Int. J. Heat Mass Transfer*, **53**(15–16), pp. 3121–3130.
- [48] Madani, B., Topin, F., Tadrist, L., and Rigollet, F., 2007, "Flow Laws in Metallic Foams: Experimental Determination of Inertial and Viscous Contribution," *J. Porous Media*, **10**(1), pp. 51–70.
- [49] Boomsma, K., Poulidakos, D., and Ventikos, Y., 2003, "Simulations of Flow Through Open-Cell Metal Foams Using an Idealized Periodic Cell Structure," *Int. J. Heat Fluid Flow*, **24**(6), pp. 825–834.
- [50] Hugo, J. M., and Topin, F., 2012, "Metal Foams Design for Heat Exchangers: Structure and Effectives Transport Properties," *Heat and Mass Transfer in Porous Media* (Advanced Structured Materials), Vol. 13, J.M.P.Q. Delgado, ed., Springer, Berlin, pp. 219–244.
- [51] Firdaous, M., Guermont, J. L., and Le Quere, P., 1997, "Nonlinear Corrections to Darcy's Law at Low Reynolds Numbers," *J. Fluid Mech.*, **343**, pp. 331–350.
- [52] Beugre, D., Calvo, S., Dethier, G., Crine, M., Toye, D., and Marchot, P., 2010, "Lattice Boltzmann 3D Flow Simulations on a Metallic Foam," *J. Comp. Appl. Math.*, **234**(7), pp. 2128–2134.
- [53] Vicente, J., Topin, F., and Daurelle, J. V., 2006, "Open-Celled Material Structural Properties Measurement: From Morphology to Transport Properties," *Mater. Trans.*, **47**(9), pp. 1–8.
- [54] Edouard, D., Lacroix, M., Huu, C. P., and Luck, F., 2008, "Pressure Drop Modelling on Solid Foam: State-of-the Art Correlation," *Chem. Eng. J.*, **144**(2), pp. 299–311.
- [55] Xu, W., Zhang, H., Yang, Z., and Zhang, J., 2008, "Numerical Investigation on the Flow Characteristics and Permeability of Three-Dimensional Reticulated Foam Materials," *Chem. Eng. J.*, **140**(1–3), pp. 562–569.
- [56] Dybbs, A., and Edwards, R. V., 1984, "A New Look at Porous Media Fluid Mechanics—Darcy to Turbulent," *Fundamentals of Transport Phenomena in Porous Media* (NATO ASI Series), Vol. 82, J. Bear, and M. Y. Corapciolu, eds., Martinus Nijhoff Publishers, Leiden, The Netherlands, pp. 199–256.
- [57] Lage, J. L., and Antohe, B. V., 2000, "Darcy's Experiments and the Deviation to Nonlinear Flow Regime," *ASME J. Fluids Eng.*, **122**(3), pp. 619–625.
- [58] Du Plessis, P., Montillet, A., Comiti, J., and Legrand, J., 1994, "Pressure Drop Prediction for Flow Through High Porosity Metallic Foams," *Chem. Eng. Sci.*, **49**(21), pp. 3545–3553.
- [59] Twigg, M. V., and Richardson, J. T., 2002, "Theory and Applications of Ceramic Foam Catalysts," *J. Chem. Eng. Res. Des.*, **80**(2), pp. 183–189.